Mathematical Analysis and Design of Carbon Nanotubes based Nantennas

by

Ashkan Vakil

Under Dr. Bajwa's supervision

Submitted to the department of Electrical Engineering
in partial fulfillment of the requirements for the degree of Master of Science in Electrical Engineering
at the

UNIVERSITY OF BRIDGEPORT

CONNECTICUT

October, 2015

The thesis "**Mathematical Analysis and Design of Carbon Nanotubes based Nantennas**" has been submitted by **Ashkan Vakil** in fulfillment of the requirements for the degree of Master of Science in Electrical Engineering. It has been approved by the thesis committee listed below:

Dr. HASSAN BAJWA (Thesis advisor and committee chairperson)

Dr. Navarun Gupta

Dr. Miad Faezipour

ABSTRACT:

Recent advances in the fabrication and characterization of nanomaterials have led to intelligible applications of such nanomaterials in next generation flexible electronics and highly efficient photovoltaic devices. Nano devices are moving on a path toward smaller designs. This idea helps scientists to extend the efficiency of nano devices such as antennas, sensors and nano robots. On the other hand, the excellent electron transport property of Graphene makes it an attractive choice for next generation electronics and applications in nanotechnology. In this paper we present a mathematically analyze of Carbon Nanotubes (CNT) based Nano antennas (Nantennas) and further we present some applications regarding to a novel design in scale of nano meter.

ACKNOWLEDGEMENTS

In advance I want to thank Dr. Bajwa for his support and kind advices toward my research and study. Without his outstanding help, academic advices and experience I could not move on the right path.

I also want to say thank you to all whom helped me reaching this point and extending my knowledge.

I appreciate my family's support and I am truly thankful from the bottom of my heart to have them in my life. They always inspire me to go on and achieve success, step by step in my life.

Table of Contents

TABLE OF FIGURES:

TABLE OF TABLES:

Chapter 1 : INTRODUCTION

1.1 Introduction

Nowadays, generating electricity is one of the most important tasks in human's life. Balancing the power generation and demand lays among highest priorities in countries' agenda [1]. Klass model is a method to approximately calculate the time takes for fossil fuels to be consumed. According to this model with some modifications, the depletion times for oil, coal and gas are about 35, 107 and 37 years, respectively [2]. Lack of fossil fuels in near future, environmental pollution caused by burning of fossil fuels, the lack of water needed in power plants, severe weather in remote places and difficulties in transmitting electricity all over the world have made us resort to distribute generation (DG) and using renewable resources instead of fossil fuels to cover the energy demand.

There are many researches going on finding a better way to produce electricity or making current method more efficient; so that we can replace it with the traditional ways. Sun radiation including heat and visible light, biomass and wind have been gathered more attention among other resources since mathematically, the amount of power that can be gathered from this resources are much higher than other renewable resources such as geothermal "Exergy is the expression for loss of available energy due to the creation of entropy in irreversible systems or processes" [3]. Exergy calculation is an important tool to see what renewable resource is more sustainable. Regarding to this, it is necessary to point out gathering the energy from sun is not as sustainable as wind or biomass heat, but since sun is more accessible in rural area, it is considered as the best renewable-based energy generation in most remote places [4]. Also one of byproducts of generating electricity with biomass is N_2O, a greenhouse gas with 100 years average global warming potential (GWP) which is about 296 times greater than same amount of CO_2 GWP [5].

Mathematical models and fabrication in this area are based on the limits of technology in previous decades. Over time, advances in technology, especially in nanotechnology area has pushed these limits more and more away. For instance, the frequency limits of diodes or other elements in electrical circuits, made us to work with a range of frequency. Now this range has been expanded and by this, we can work in higher energy range:

$$E\ (j) = h\ (j.s) \times f\ (Hz) \qquad \text{(Equation 1)}$$

Where "E" is energy (j), "h" is plank's constant (6.62×10^{-34} j.s) and "f" is the frequency (Hz).

By these advancements, there are significant improvements in converters, inverters, switches and other fundamental devices that are used in mentioned power generation method. Another example is the wind turbines. Recent advancements in rotors, control systems, electronics circuits and gearboxes of windfarms, have led us to achieve better efficiency in output power.

1.2 Sun, the biggest energy source in the Solar System:

The Sun is located in the center of our solar system and other stars in solar system orbit the Sun. it is known as the biggest energy source in Solar System. Sun's energy is being released in the form of sunlight with varied frequency range. This energy supports almost all life on Earth. The Sun is composed of hydrogen (about 74% of its mass, or 92% of its volume), helium (about 25% of mass, 7% of volume), and small amount of other elements. It has a surface temperature of approximately 5500 (K). Sunlight is the main source of energy to the surface of Earth. The solar constant, which is the amount of power Sun irradiance per unit area, is about 1370 watts per square meter of area at a distance of one Astronomic Unit (AU) from the Sun (that is, on or near Earth). Although sunlight is attenuated by the Earth's atmosphere while it is reaching the surface, it is almost about 1000 watts per directly exposed square meter in clear conditions when the Sun is near the zenith.

About 3.4×10^{38} protons (hydrogen nuclei) are converted into helium nuclei every second (out of about $\sim 8.9 \times 10^{56}$ total amount of free protons in Sun) via fusion reaction. Byproduct is releasing as energy at the matter-energy conversion rate of 4.26 million tons per second, 383 Yottawatts (383×10^{24} W) or 9.15×10^{10} megatons of TNT per second [6]. This energy releases in the form of electromagnetic waves (photons). Irradiation of photons from sun with different frequency causes the heat and appearance of light on earth. Even wind blows because of the heat of the sun.

Chapter 2 : CARBON NANOTUBES

2.1 CNT Review:

Carbon can bond in many ways to create different structure with different properties. It is because of its chemical characteristics. Carbon has four valance electrons. Sharing these electrons in different ways ends to different structures. For instance when all four electrons are shared equally, it creates diamond, an isotropically strong structure; while if only three electrons are shared in covalence bond between neighbors in a plane and forth electron is allowed to move among all atoms, it makes graphite [7]. Graphene is another formation of carbon atoms, which is single layer, and it has lattice honeycomb structure.

Early experiments in the mid-1980s, which leaded to the fullerene discovery, presented that when the number of carbon atoms is smaller than a few hundred, the structures formed correspond to linear chains, rings, and closed shells [7], [8]. "The fullerenes are closed shell carbon based structure with an even number of atoms (starting at C_{28}, which has been observed by mass spectrometers in carbon soot) and nominal sp^2 bonding between adjacent atoms" [7]. To form curved structures, such as the fullerenes, from a planar fragment of hexagonal graphite lattice, we have to include specific topological defects in the structure. In order to produce a convex formation, positive curvature has to face the planar hexagonal graphite lattice. Creating pentagons can do this. A greatly elongated fullerene can be formed with exactly 12 pentagons and millions of hexagons [9]. This would correspond to a carbon nanotube [7], [9]. Tube's diameter will rely on the size of the semi-fullerene which the end is made of [7], [9].

If we somehow fold a graphene sheet into a cylinder such that the open edges match perfectly to form a seamless structure, result will be an open ended tube." The tubes have to be closed at both ends, which means that at some stage in the growth process pentagons are nucleated to initiate the closure mechanism"[7].

Nanotubes structures are divided in two categories. First are called the multi-walled carbon nanotubes (MWNT) were the first to be discovered. Second are called the single-walled carbon nanotubes (SWCNT) which possess good uniformity in diameter (1-2 nm)" [7].

2.2 CNT Lattice structure:

CNTs are cylinder formation of Carbon atom and regarding to their binding types and characteristics of Carbon atoms, they are considered among highly conductive materials. Nantenna fabrication with the use of CNT as the base material of Nantenna attracts researchers' attention since the high conductivity of CNT increases the efficiency of Nantenna; however putting CNTs in specific form is not easy. Later we mathematically analyze CNT conductivity. Nowadays, CNT and Graphene are being used in many applications and nano devices such as transistors and Nantennas. Energy harvesting via renewable resources is changing to be a big pole of future industry since the traditional way of producing electricity will face fundamental issues in future. Using these Nantennas might be a good replacement for typical solar panels.

CNTs are nothing more than rolled up graphene sheets along the chiral vector. In we somehow cut the CNT and spread it, the chiral vector is the vector that shows the opened circumference of CNT (figure 1).

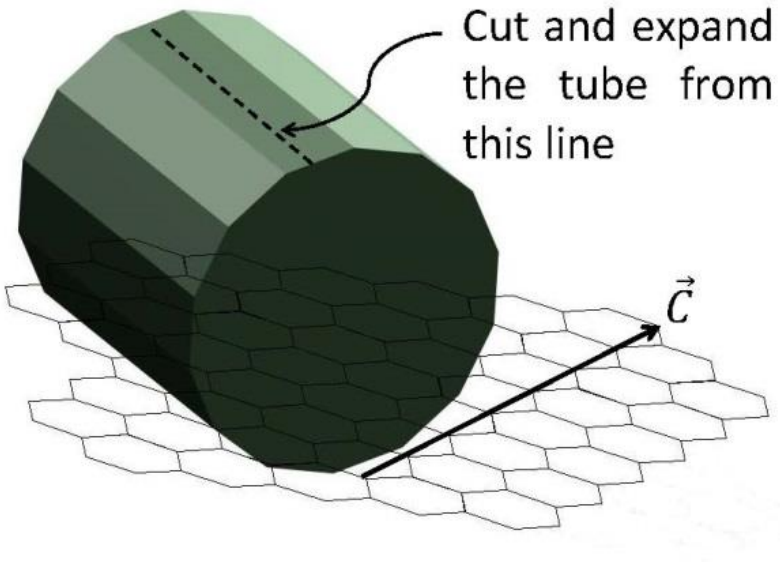

Figure 1 : Chiral vector demonstration

Since the foundation of CNT is graphene sheets, the best way for analyzing CNT is to analyze graphene. Graphene is a mono-layered honeycomb crystal of carbon atoms (figure 2). It has two sub-lattices, which are separated with black and white circles in figure 2.

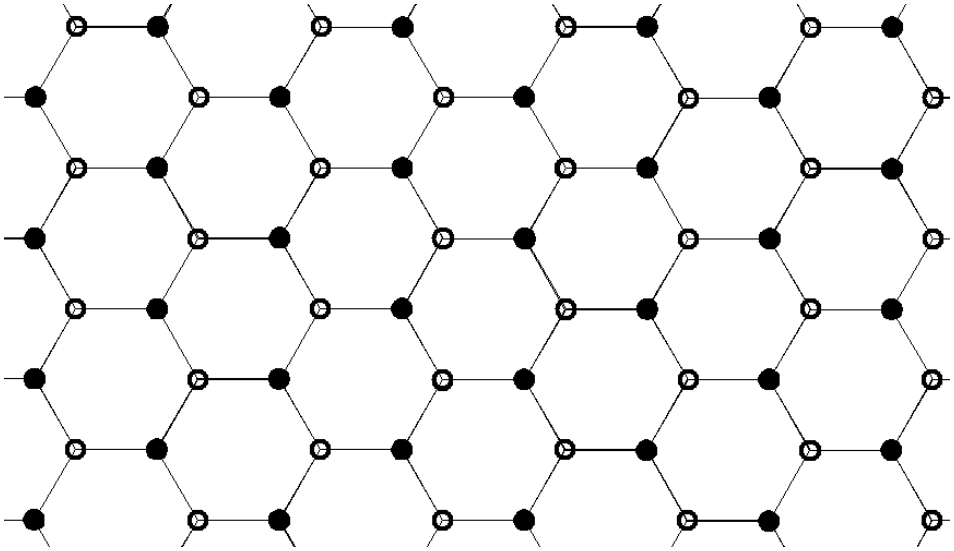

Figure 2 : Graphene honeycomb lattice structure. Sublattices are seperated with bullet points and circles

In order to analyze graphene's structure, we define the unit cell as a rhombus shape which contains one atom from each sublatice. It is shown in figure 3.

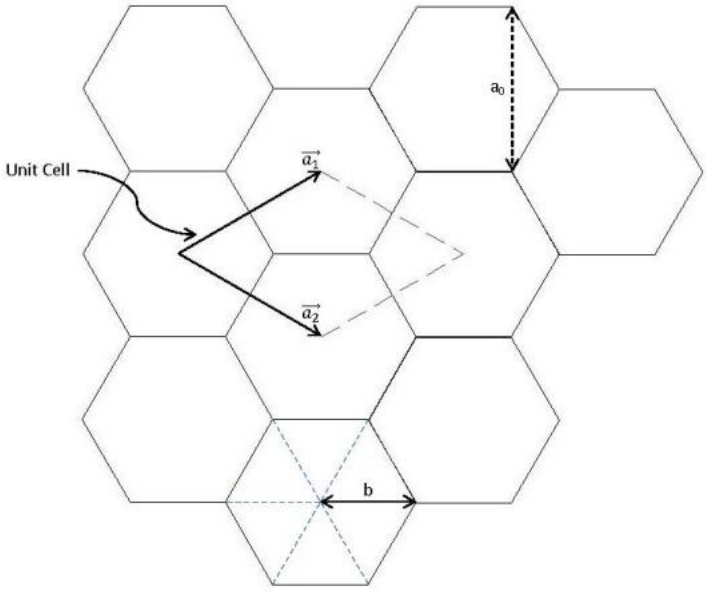

Figure 3 : Graphene Unit Cell

As it is shown in figure 3, unit cell can be defined with two vectors, "$\overrightarrow{a_1}$" and "$\overrightarrow{a_2}$":

$$\overrightarrow{a_1} = (\frac{\sqrt{3}\, a_0}{2}, \frac{a_0}{2}) \quad \text{(Equation 2)}$$

$$\overrightarrow{a_2} = (\frac{\sqrt{3}\, a_0}{2}, \frac{-a_0}{2}) \quad \text{(Equation 3)}$$

Where:

$$|a_1| = |a_2| = a_0 = \sqrt{3} b_0 \quad \text{(Equation 4)}$$

"b_0" is the interatomic distance in the lattice structure which is 0.142 (nm).

As it is mentioned in chiral vector's definition, in two dimensions, the circumference of opened CNT can be shown with the chiral vector (C):

$$\vec{C} = n\overrightarrow{a_1} + m\overrightarrow{a_2} \quad \text{(Equation 5)}$$

Different "*n"* and "*m"* causes different edge types in the CNT containing zigzag, armchair and chiral CNTs:

$$\begin{cases} zigzag & m = 0 \\ armchair & m = n \\ chiral & O.W. \end{cases} \quad \text{(Equation 6)}$$

Also, "*m"* and "*n"* show whether the SWCNT is metallic or semiconductor as if (n-m)/3 is equal to an integer, CNT is metallic, and otherwise it is semiconductor. Metallic ones have high conductivity which makes current density be able to reach 4×10^9 A/cm^2. This high conductivity put CNTs in the top of high conduction materials such as copper. All armchair CNTs are metallic. In contrary, only one third of zigzag CNTs are metallic, so in general approximately one third of CNTs are metallic.

Circumference of CNT can be found by:

$$|c| = \sqrt{|na_1|^2 + |ma_2|^2 + 2|na_1 ma_2| \cos\theta} \quad \text{(Equation 7)}$$

Where:

$$\theta = 60^{\circ} \quad \text{(Equation 8)}$$

So:

$$|c| = \sqrt{|na_1|^2 + |ma_2|^2 + |na_1 ma_2|} \quad \text{(Equation 9)}$$

From equations 4 and 9 we have:

$$|c| = a_0\sqrt{n^2 + m^2 + nm} \quad \text{(Equation 10)}$$

So radius of CNT is:

$$r_{CNT} = \frac{|c|}{2\pi} = \frac{a_0}{2\pi}\sqrt{n^2 + m^2 + nm} \quad \text{(Equation 11)}$$

2.3 CNT Conductivity:

Conductivity in nano scales has different scenario. In bigger scale, we consider electron's transportation as diffusive transportation, which means electron does not move in just one path to reach its destination. The reason is that since distances are much greater than atomic scale, electron might hit other atomic objects in its way and moves in random directions and the summation of these movements is a straight displacement. In contrary, in nano scale, since distances are close to atomic scale (a little less than one nano meter), electron moves on a single path and we can consider the transportation straight with a good approximation. This type of transportation is called Ballistic transportation, since electrons move like bullets.

We cannot implement the common conductivity equation ($\sigma = \left(\rho \frac{L}{A}\right)^{-1}$) to find the conductivity in nano scale. If we consider the common equation, since "L" tends to be zero, the conductivity would become infinity and it is against results in nano scale experiments. In order to find the conductivity, we should analyze changes in electrons energy (electrons movements). We use the Boltzmann transport equation for this purpose:

$$\frac{\partial f}{\partial t} + eE_z \frac{\partial f}{\partial p_z} + v_z \frac{\partial f}{\partial z} = \vartheta[f_0(p) - f] \quad \text{(Equation 12)}$$

Where "e" is electrons charge, "E_z" is the longitudinal component of the electric field at the nanotube surface, "v_z" is electron's velocity, "ϑ" is the relaxation frequency and "$f_0(p)$" is the Fermi-Dirac distribution equation which is a function of electron's momentum. "f" is electron's distribution function:

$$f = f(p,z,t) = f_0(p) + Re\left(\delta f e^{j\omega t}\right) \quad \text{(Equation 13)}$$

The Fermi-Dirac distribution relation can be written as:

$$f_0(p) = \left(1 + e^{\frac{E(p)-E_F}{k_B T}}\right)^{-1} \quad \text{(Equation 14)}$$

Where "$E(p)$" is the energy-momentum relation, "E_F" is Fermi energy, "k_B" is the Boltzmann constant and "T" is nanotube absolute temperature. Fermi energy in graphene is zero. Considering the longitudinal component of the electric field as:

$$E_z = Re\left(\hat{E}_z e^{j\omega t}\right) \quad \text{(Equation 15)}$$

Then we can write:

$$f = f_0(p) + \delta f \cos(\omega t) \quad \text{(Equation 16)}$$

$$E_z = \hat{E}_z \cos(\omega t) \quad \text{(Equation 17)}$$

Putting results in equation 12 leads to:

$$-\delta f \omega \sin(\omega t) + e\hat{E}_z \cos(\omega t)\frac{\partial f_0}{\partial p_z} = \vartheta[f_0(p) - f_0(p) - \delta f \cos(\omega t)] \quad \text{(Equation 18)}$$

$$\delta f = j\frac{\partial f_0}{\partial p_z}\frac{e\hat{E}_z}{\omega - j\vartheta} \quad \text{(Equation 19)}$$

The axial current density in two dimensional lattice structures can be shown as:

$$J_z = \frac{2e}{(2\pi\hbar)^2}\sum_{p\emptyset}\int_{first\ Brillion\ zone} v_z f dp_z \quad \text{(Equation 20)}$$

Where

$$J_z = Re(\hat{J}_z e^{j\omega t}) \quad \text{(Equation 21)}$$

And

$$\hat{J}_z = \sigma_{zz}(\omega)\hat{E}_z \quad \text{(Equation 22)}$$

So, from above equations, we have:

$$\sigma_{zz}(\omega) = j\frac{2e^2}{(2\pi\hbar)^2}\sum_{p_\emptyset}\int_{first\ Brillion\ zone}\frac{\partial f_0(p)}{\partial p_z}\frac{v_z}{(\omega - j\vartheta)}dp_z \quad \text{(Equation 23)}$$

Where the summation is in the first Brillion zone of SWCNT where it is [10]:

$$\begin{cases} |P_\emptyset| = \frac{s}{m}\frac{2\pi\hbar}{\sqrt{3}a_0}, \quad s = 1,2,3,\dots,m \\ |P_z| < \frac{4\pi\hbar}{3a_0} - \frac{1}{\sqrt{3}}P_\emptyset \end{cases} \quad \text{(Equation 24)}$$

Where "s" accounts for the quantized momentum in the circumferential direction [11]. "m" is from Chiral vector (equation 5).

In order to solve this equation, we need to find the energy-momentum relation in graphene and for this concept; we need to analyze the energy band, which requires using Schrodinger time independent equation.

2.4 Energy Band

Experiments showed Newtonian Mechanics is inaccurate in atomic distance. Schrodinger presented an equation for both microscopic and macroscopic universes called the "wave equation". Since electrons have fixed total energy, we should use the time independent Schrodinger equation in order to analyze CNT. From Schrodinger time independent equation:

$$E\psi = \frac{-\hbar}{2m}\nabla^2\psi + U(\vec{r})\psi \quad \text{(Equation 25)}$$

Or we can write it like:

$$E\psi = \{\frac{-\hbar}{2m}\nabla^2 + U(\vec{r})\}\psi \quad \text{(Equation 26)}$$

"ψ" is called the "wave function" which is function of space coordinates and time. Since we are using time independent Schrodinger equation, we do not consider the time part of "ψ". "ψ" shows the location of electron. "*m"* is mass of electron in vacuum, "$\hbar$" is reduced plank constant and "$U(\vec{r})$" is potential energy. The equation is fit for vacuum condition; but in solid objects, like Graphene, electron behaves almost as if it is in vacuum but with different mass. We call this mass Effective Mass Equation (EME). So we just replace electron mass in the equation with "m_{eff}":

$$E\psi = \{\frac{-\hbar}{2m_{eff}}\nabla^2 + U(\vec{r})\}\psi \qquad \text{(Equation 27)}$$

The reason convinces us to agree with this equation, is that Schrodinger was able to solve this equation for electron in Hydrogen atoms and confirm it with experimental results. From experiment, it was shown that electrons in Hydrogen atoms have certain discrete energy levels. This could be resulted by observing the light emitted from Hydrogen atom while it is heated. Frequencies of this lights corresponded to this different energy level. On the other hand, Schrodinger showed by solving this equation for electrons in Hydrogen atoms, using the electron potential energy ($\frac{-q^2}{4\pi\varepsilon_0 r}$), we end up with solutions for energy with specific discrete values, the eigenvalues. This means energy resulted from analytically solution of Schrodinger equation could not be something else except eigenvalues [12].

Although Schrodinger was able to solve this equation for Hydrogen atom analytically, there are very few practical examples that can be solved analytically. Most of them need to be solved via numerical solution; like the way computers solving equation. In this case, we should turn the differential equation into matrix equation. Since Graphene has two-dimensional structure, elements in equation will be two by two matrixes. By presenting the differential operator as H_{op}:

$$H_{op} = \frac{-\hbar}{2m}\nabla^2 + U(\vec{r}) \qquad \text{(Equation 28)}$$

We can change the differential Schrodinger equation into matrix form by changing elements to matrixes as:

$$E[S]\{\psi\} = [H]\{\psi\} \qquad \text{(Equation 29)}$$

Where braces present column vector and brackets presents matrix. The column vector of {ψ} can be found by writing the $\psi_{(\vec{r})}$as linear combination of the data we know:

$$\psi_{(\vec{r})} = \psi_1 u_{1(\vec{r})} + \psi_2 u_{2(\vec{r})} + \cdots = \sum_n \psi_n u_{n(\vec{r})} \quad \text{(Equation 30)}$$

$\psi_{(\vec{r})}$ is the function that we do not know and we write it as a set of functions we do know ($u_{n(\vec{r})}$) and coefficients (ψ_n). So column vector, {ψ}, can be presents as:

$$\{\psi\} = \begin{Bmatrix} \psi_1 \\ \psi_2 \\ \vdots \end{Bmatrix} \quad \text{(Equation 31)}$$

We are using the semi-empirical method to write matrixes S and H. it means instead of finding the elements of matrixes S and H via Gaussian equation, we just adjust the parameters, to make sure it matches well-known results for material that we are interested here, which means Graphene. So we assume S matrix is an identity matrix. So we can drop S matrix from our equation;

$$E\{\psi\} = [H]\{\psi\} \quad \text{(Equation 32)}$$

Then we will find H as it leads to result that matches well-known theoretical results or experimental observations. We find it with the use of "nearest neighbor model" method which means we choose the interaction of non-neighbor atoms to be zero.

So in the process of changing the differential equation to matrix equation, we are replacing the differential operation function (H_{op}) with matrix H. matrix H is called Hamiltonian matrix. Since these two equations are the same, it is obvious that the answers should be the same.

ψ_n can be represented as:

$$\{\psi_n\} = \{\psi_\circ\} e^{i\vec{k}.\vec{r}_n} \quad \text{(Equation 33)}$$

Where r_n is position vector of n^{th} atom, which shows the vector started from first atom toward the other atom. Since our Graphene structure is two dimensional, vector $\vec{k}$ has two elements containing $\vec{x}$ and $\vec{y}$ elements. Also E is going to be a function of $\vec{k}$.

From equation 32 we will have:

$$E\begin{Bmatrix}\psi_1\\ \psi_2\\ \vdots\end{Bmatrix}=\begin{bmatrix}H_{11} & \dots & H_{1n}\\ \vdots & \ddots & \vdots\\ H_{m1} & \dots & H_{mn}\end{bmatrix}\begin{Bmatrix}\psi_1\\ \psi_2\\ \vdots\end{Bmatrix} \qquad \text{(Equation 34)}$$

Or simpler for each element in matrix:

$$E\{\psi_n\}=\sum_{m=1}^{n}[H_{nm}]\{\psi_m\} \qquad \text{(Equation 35)}$$

From above equations:

$$E(\vec{k})\{\psi_\circ\}=\sum_m[H_{nm}]e^{i\vec{k}(\vec{r_m}-\vec{r_n})}\{\psi_\circ\} \qquad \text{(Equation 36)}$$

As is it mentioned before, Graphene has a two-dimensional lattice structure. In order solve the Schrodinger equation for Graphene (or any other structures) we need to define a unit cell in which the whole structure can represent with that by just copy it continuously. We choose the unit cell as:

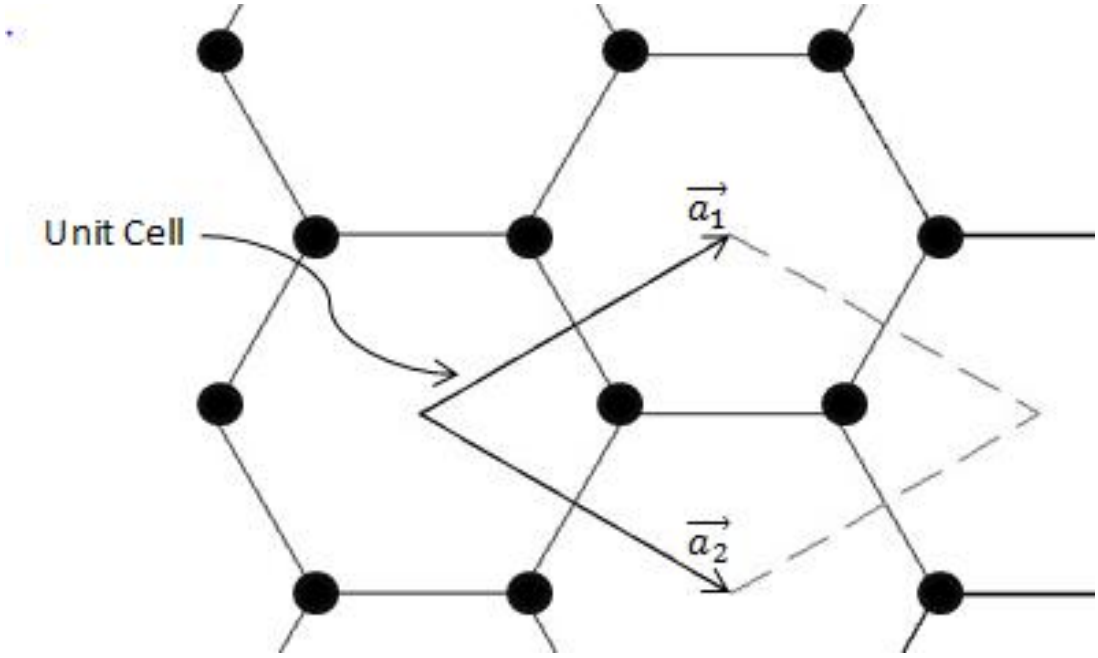

Figure 4 : Graphene's unit cell. $\overrightarrow{\boldsymbol{a_1}}$ and $\overrightarrow{\boldsymbol{a_2}}$are basic vectors of unit cell

So each unit cell contains of two atom so ψ◦ is going to be a matrix. Since ψ◦ is a matrix, we cannot cancel it from both sides. Also $[H_{nm}]$ is going to be a two by two matrix. We can find the energy eigenvalue, by finding the eigenvalue of $\left[h(\vec{k})\right]$ where:

$$\left[h(\vec{k})\right] = \sum_m [H_{nm}] e^{i\vec{k}(\overrightarrow{r_m} - \overrightarrow{r_n})} \qquad \text{(Equation 37)}$$

Now for writing $\left[h(\vec{k})\right]$ we should use the nearest neighbor model. In order so, we will pursue by analyzing Graphene structure diagram and unit cell in six steps.

2.4.1 First, unit cell and itself:

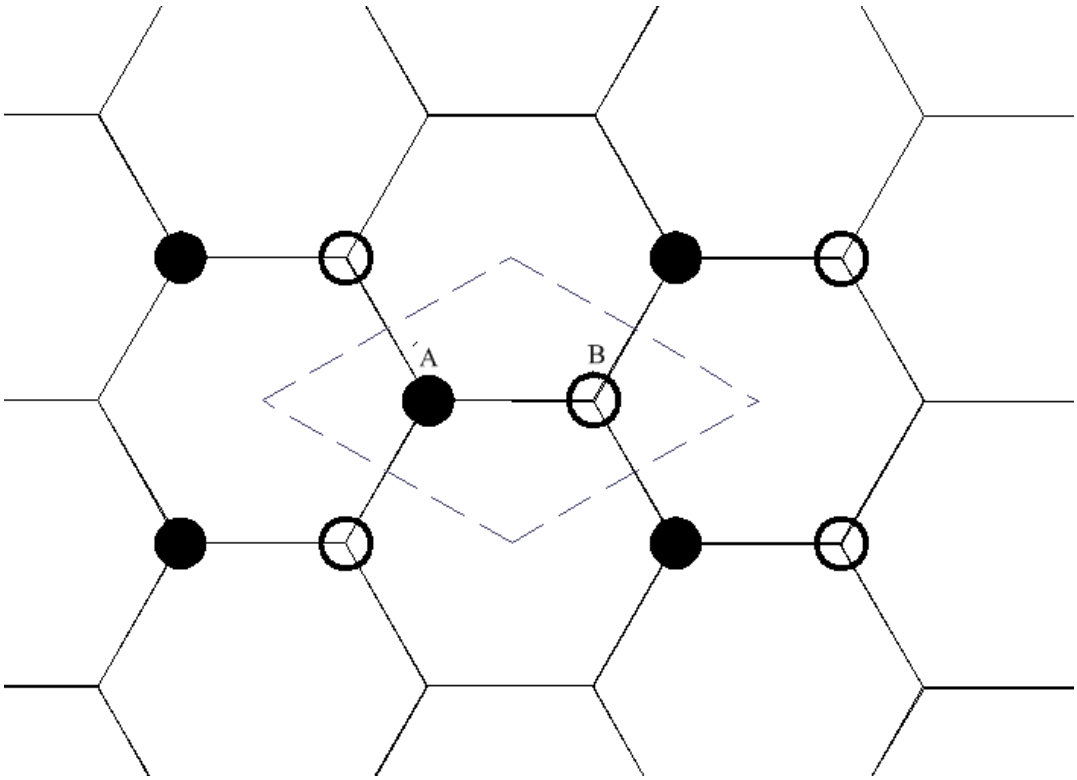

Figure 5 : First step of the nearest neighbor model

In this case n=m. first parameter is the relation of atom A with itself. We show it with "ε". Second parameter is the relation between A and B, since they are neighbor atoms; it is a non-zero

value, which can be shown with "γ". Third parameter is relation between atom B and atom A, which is also "γ". Last parameter is relation between atom B and itself so it is "ε". So the corresponding matrix is going to be:

$$[H_{nn}] = \begin{bmatrix} \varepsilon & \gamma \\ \gamma & \varepsilon \end{bmatrix} \quad \text{(Equation 38)}$$

So when n=m;

$$[H_{nm}]e^{i\vec{k}(\overrightarrow{r_m}-\overrightarrow{r_n})} = [H_{nn}]e^{i\vec{k}(\overrightarrow{r_n}-\overrightarrow{r_n})} = \begin{bmatrix} \varepsilon & \gamma \\ \gamma & \varepsilon \end{bmatrix} e^0 = \begin{bmatrix} \varepsilon & \gamma \\ \gamma & \varepsilon \end{bmatrix} \quad \text{(Equation 39)}$$

2.4.2 Second, unit cell and its top left neighbor:

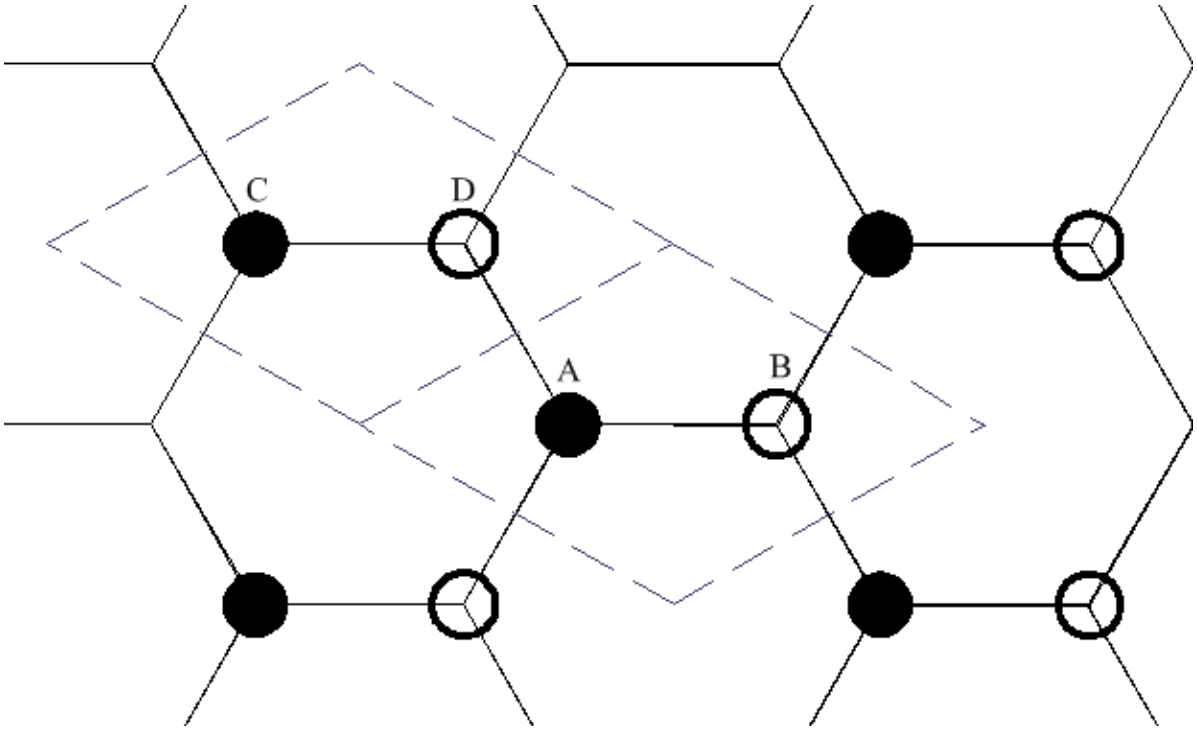

Figure 6 : Second step of the nearest neighbor model

In this case mth unit cell is located on top-left side. First parameter is the relation between atoms A with atom C, since they are not neighbors, the parameter is zero. Second parameter is the relation between A and D, since they are neighbor atoms; it is a non-zero value, which can be shown with

"γ". Third parameter is relation between atom B and atom C, which is zero. Last parameter is relation between atom B and atom D and it is also zero. So the corresponding matrix is going to be:

$$[H_{nm}] = \begin{bmatrix} 0 & \gamma \\ 0 & 0 \end{bmatrix} \quad \text{(Equation 40)}$$

So:

$$[H_{nm}] e^{i\vec{k}(\overrightarrow{r_m} - \overrightarrow{r_n})} = \begin{bmatrix} 0 & \gamma \\ 0 & 0 \end{bmatrix} e^{-i\vec{k}\overrightarrow{a_2}} \quad \text{(Equation 41)}$$

Where $\overrightarrow{a_2}$ is unit cells vector.

2.4.3 Third, unit cell and its top right neighbor:

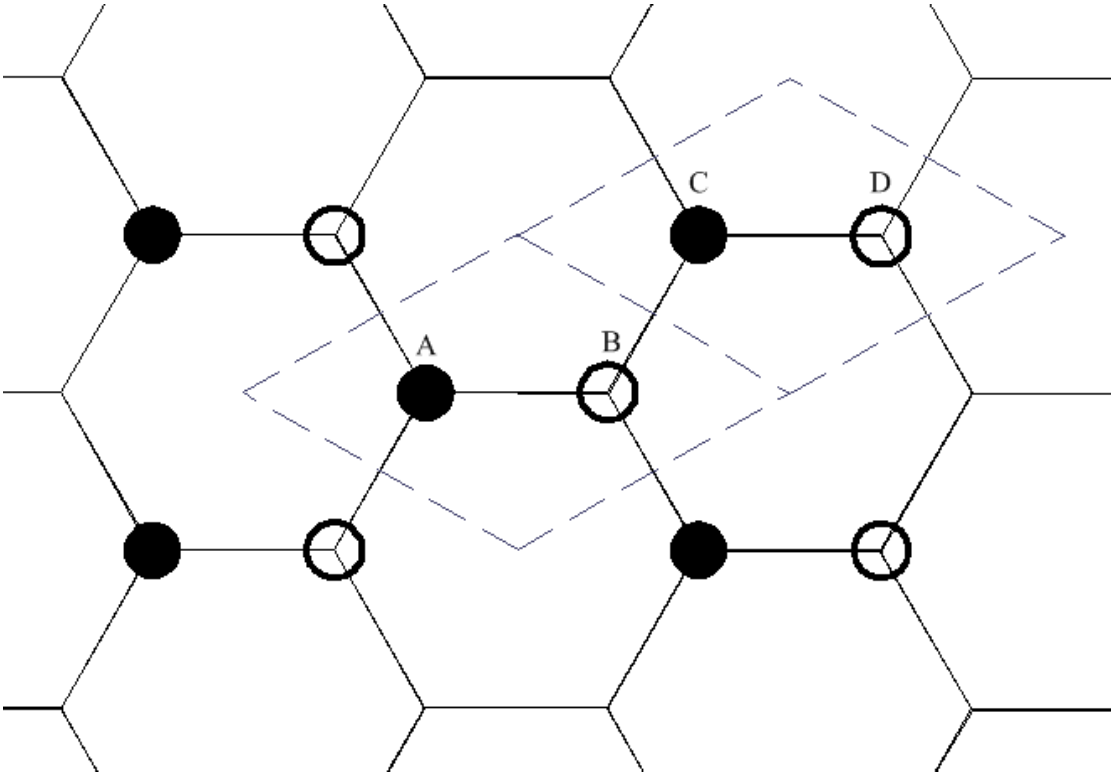

Figure 7 : Third step of the nearest neighbor model

In this case m[th] unit cell is located on top-right side. First parameter represents the relation between atoms A with atom C and since they are not neighbors, this parameter is zero. Second parameter is the relation between A and D, since they are not neighbors atoms, the parameter is zero. Third parameter is relation between atom B and atom C, which is "γ". Last parameter is relation between atom B and atom D and it is zero. So the corresponding matrix is going to be:

$$[H_{nm}] = \begin{bmatrix} 0 & 0 \\ \gamma & 0 \end{bmatrix} \quad \text{(Equation 42)}$$

So:

$$[H_{nm}] e^{i\vec{k}(\overrightarrow{r_m} - \overrightarrow{r_n})} = \begin{bmatrix} 0 & 0 \\ \gamma & 0 \end{bmatrix} e^{+i\vec{k}\overrightarrow{a_1}} \quad \text{(Equation 43)}$$

Where $\overrightarrow{a_1}$ is unit cells vector.

2.4.4 Forth, unit cell and its bottom left neighbor:

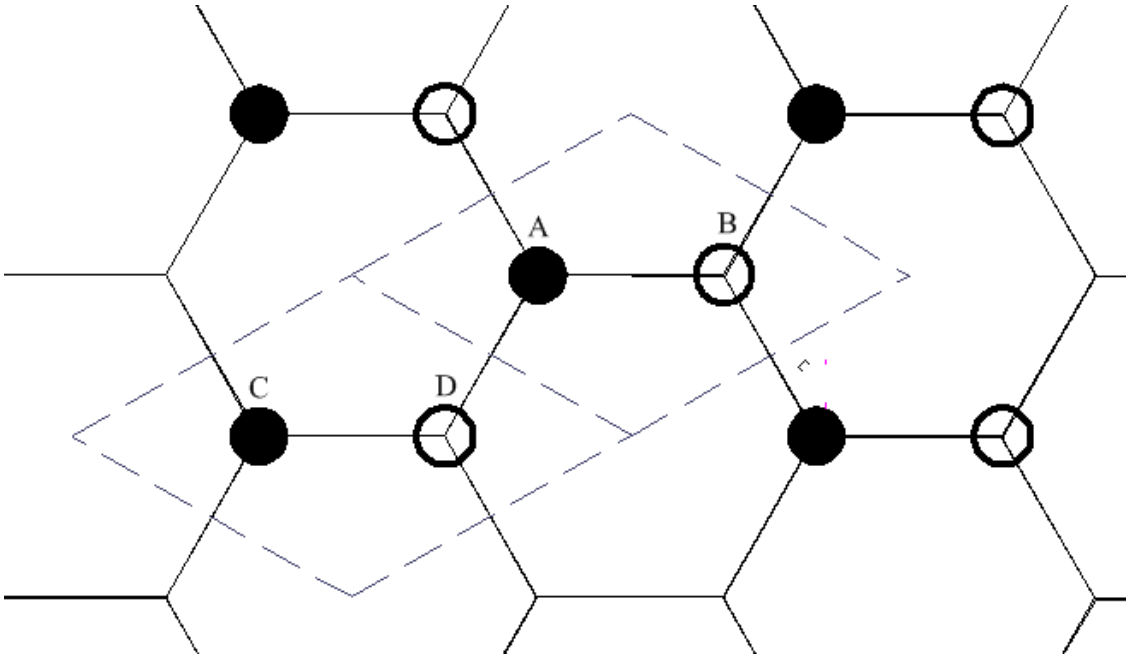

Figure 8 : Forth step of the nearest neighbor model

In this case m[th] unit cell is located on bottom-left side. First parameter is the relation between atoms A with atom C, since they are not neighbors, the parameter is zero. Second parameter is the

relation between A and D, since they are neighbor atoms; it is a non-zero value, which can be shown with "γ". Third parameter is relation between atom B and atom C, which is zero. Last parameter is relation between atom B and atom D and it is also zero. So the corresponding matrix is going to be:

$$[H_{nm}] = \begin{bmatrix} 0 & \gamma \\ 0 & 0 \end{bmatrix} \quad \text{(Equation 44)}$$

So:

$$[H_{nm}]e^{i\vec{k}(\vec{r_m}-\vec{r_n})} = \begin{bmatrix} 0 & \gamma \\ 0 & 0 \end{bmatrix} e^{-i\vec{k}\vec{a_1}} \quad \text{(Equation 45)}$$

2.4.5 Fifth, unit cell and its bottom right neighbor:

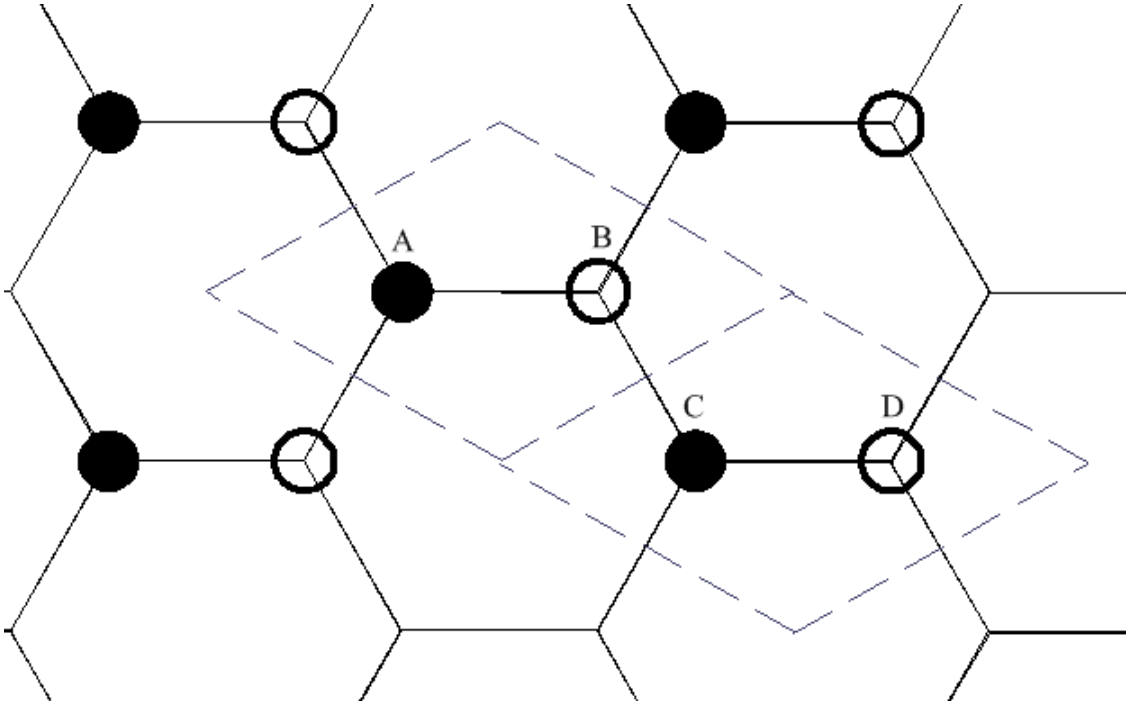

Figure 9 : Fifth step of the nearest neighbor model

In this case m^{th} unit cell is located on bottom-right side. First parameter is the relation between atoms A with atom C, since they are not neighbors, the parameter is zero. Second parameter is the

relation between A and D, since they are not neighbors atoms, the parameter is zero. Third parameter is relation between atom B and atom C, which is "γ". Last parameter is relation between atom B and atom D and it is zero. So the corresponding matrix is going to be:

$$[H_{nm}] = \begin{bmatrix} 0 & 0 \\ \gamma & 0 \end{bmatrix} \quad \text{(Equation 46)}$$

So:

$$[H_{nm}]e^{i\vec{k}(\overrightarrow{r_m}-\overrightarrow{r_n})} = \begin{bmatrix} 0 & 0 \\ \gamma & 0 \end{bmatrix} e^{+i\vec{k}\overrightarrow{a_2}} \quad \text{(Equation 47)}$$

2.4.6 Sixth, summation of each element:

In order to write the $\left[h\left(\vec{k}\right)\right]$:

$$\left[h\left(\vec{k}\right)\right] = \sum_m [H_{nm}]e^{i\vec{k}(\overrightarrow{r_m}-\overrightarrow{r_n})} = \begin{bmatrix} \varepsilon & \gamma\left(1 + e^{-i\vec{k}\overrightarrow{a_1}} + e^{-i\vec{k}\overrightarrow{a_2}}\right) \\ \gamma\left(1 + e^{i\vec{k}\overrightarrow{a_1}} + e^{i\vec{k}\overrightarrow{a_2}}\right) & \varepsilon \end{bmatrix}$$

(Equation 48)

Assuming that

$$h_0 = \gamma\left(1 + e^{i\vec{k}.\vec{a}_1} + e^{i\vec{k}.\vec{a}_2}\right) \quad \text{(Equation 49)}$$

Then we have:

$$h\left(\vec{k}\right) = \begin{bmatrix} \varepsilon & {h_0}^* \\ h_0 & \varepsilon \end{bmatrix} \quad \text{(Equation 50)}$$

Using equations 2, 3 and 49:

$$h_0 = \gamma(1 + e^{i\vec{k}.(\frac{\sqrt{3}}{2}a_0\hat{x} + \frac{1}{2}a_0\hat{y})} + e^{i\vec{k}.(\frac{\sqrt{3}}{2}a_0\hat{x} - \frac{1}{2}a_0\hat{y})}) \quad \text{(Equation 51)}$$

Assuming $\vec{k}.\hat{x} = k_x$ and $\vec{k}.\hat{y} = k_y$, we can simplify the equation and find $|h_0|$ as:

$$|h_0| = -\gamma\sqrt{1 + 4\cos^2(\frac{a_0}{2}k_y) + 4\cos(\frac{\sqrt{3}}{2}a_0k_x)\cos(\frac{a_0}{2}k_y)} \quad \text{(Equation 52)}$$

Mathematical review for eigenvalue:

In order to find the eigenvalue of matrix $[h(\vec{k})]$:

$$\lambda I = \lambda \begin{bmatrix} 1 & 0 \\ 0 & 1 \end{bmatrix} = \begin{bmatrix} \lambda & 0 \\ 0 & \lambda \end{bmatrix} \quad \text{(Equation 53)}$$

$$h(\vec{k}) - \lambda I = \begin{bmatrix} \varepsilon - \lambda & {h_0}^* \\ h_0 & \varepsilon - \lambda \end{bmatrix} \quad \text{(Equation 54)}$$

Now, by solving below equation, eigenvalue will be "λ":

$$\begin{vmatrix} \varepsilon - \lambda & {h_0}^* \\ h_0 & \varepsilon - \lambda \end{vmatrix} = 0 \Longrightarrow$$

$$(\varepsilon - \lambda)^2 - |h_0|^2 = 0 \Longrightarrow$$

$$\lambda = \varepsilon \pm |h_0| \quad \text{(Equation 55)}$$

So, the eigenvalue will be:

$$\varepsilon \pm |h_0| \quad \text{(Equation 56)}$$

So, the energy momentum relation for Graphene can be written as:

$$E = \varepsilon \pm |h_0| \quad \text{(Equation 57)}$$

It means for each "$\vec{k}$" we will have two eigenvalues; from experiments "ε" can be obtained and it is equal to zero [13]; so:

$$E = -\gamma \sqrt{1 + 4\cos^2(\frac{a_0}{2}k_y) + 4\cos(\frac{\sqrt{3}}{2}a_0 k_x)\cos(\frac{a_0}{2}k_y)} \quad \text{(Equation 58)}$$

Below is the plot of energy-momentum relation:

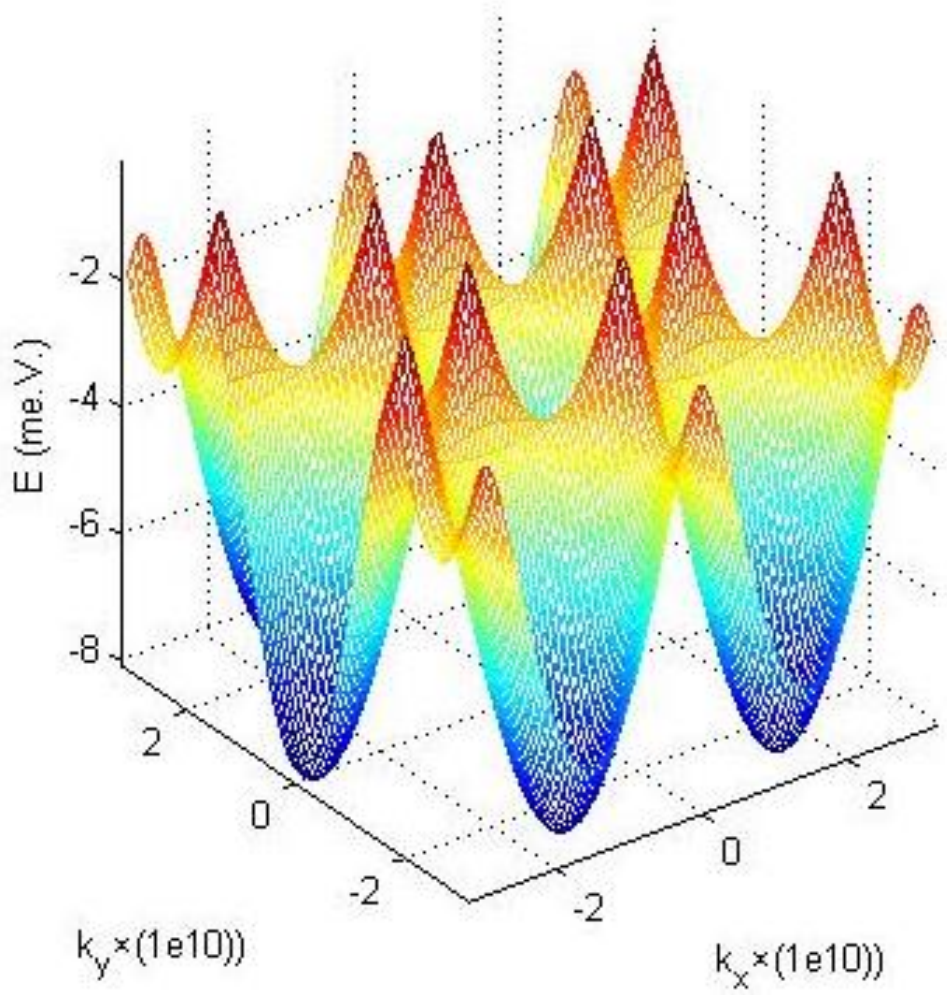

Figure 10 : Energy-momentum relation in first Brillion zone

MATLAB codes for the plot are attached in appendix A.

In order to make the plot more tangible, "a_0" is divided by 10^{10} in the plotting procedure.

Assuming $\vec{k}.\hat{x} = k_x$ and $\vec{k}.\hat{y} = k_y$, and regarding to the relation between "$\vec{k}$" and "**P**" as bellow:

$$k_y = \frac{P_z}{\hbar} \qquad \text{and} \qquad k_x = \frac{P_\emptyset}{\hbar} \qquad \text{(Equation 59)}$$

We can write the energy-momentum relation as:

$$E_{(P)} = -\gamma\sqrt{1 + 4\cos^2(\frac{a_0}{2\hbar}P_z) + 4\cos(\frac{\sqrt{3}}{2\hbar}a_0P_\emptyset)\cos(\frac{a_0}{2\hbar}P_z)} \qquad \text{(Equation 60)}$$

Wherein "γ" is the overlap energy and it is equal to 2.7e.V. [13], [14].

Chapter 3 APPLICATIONS:

Nanotechnology and nanoparticles based devices are thriving research areas. The last decade has seen as increase use of nanotechnology in sensors, biomedical and medicine applications [15], [16]. CNT and nano-wires based technology have also been used in radio-frequency, microwave, power harvesting and bioelectronics [17]–[19]. Having a conductive DNA would be enormously useful since it makes it possible to create conductive Nantennas and sensor in different shapes in such small scale.

Self-assembling 3-D DNA structures combined with carbon nanotube (CNT) based nanotechnology have the potential to revolutionize nano-electronics and biomedical. Bottom-up growth of self-assembled technology have enabled researchers to build nanoscale structures, like Nantenna, with sound electrical and thermal properties [20], [21]. Conductivity of such a biological Nantenna can be achieved by using conductive nanoparticles coating on DNA [22] or by attaching nanowire to DNA structures [23]. Recent advances in nanotechnology and the synthesis of scaffold based nanostructures have led to the possibility of realizing nanoscale devices cost-effectively [24].

Fabricating DNA scaffold based nanoscale- spiral Nantenna with CNT can be used in energy harvesting applications. Presented idea is also published as conference paper which is attached to the end of this thesis. Sun's energy, conventionally, gathered by solar Photovoltaic (PV) panels. They convert the energy of photons with infrared and visible light frequency band into electrical energy via two procedures, one physical and the other chemical. According to equation 1, gathering the energy of photons with higher frequency leads to produce more energy.

Wave	Frequency range	Energy of a photon (e.V.)
Infrared	0.3THz – 0.429 PHz	0.001 – 1.772
Visible-Light	0.385PHz – 0.789 PHz	1.591 – 3.265
UV-A	0.75 PHz – 0.952 PHz	3.102 – 3.939
UV-B	0.952 PHz – 1.07 PHz	3.939 – 4.431
UV-C	1.07 PHz – 1.5 PHz	4.431 – 6.203
Vacuum UV	1.5 PHz – 3 PHz	6.203 – 12.407

Table 1 : List of the energy of photons with different frequencies [25]

Another factor is the density of photons with desired frequency. This can be realized via irradiance for each frequency. Taking a look at the irradiance of each frequency makes it easier to choose Nantenna's size. Irradiance data are collected by Solar Radiation and Climate Experiment (SORCE) from Laboratory for Atmospheric and Space Physics of the University of Colorado [26]:

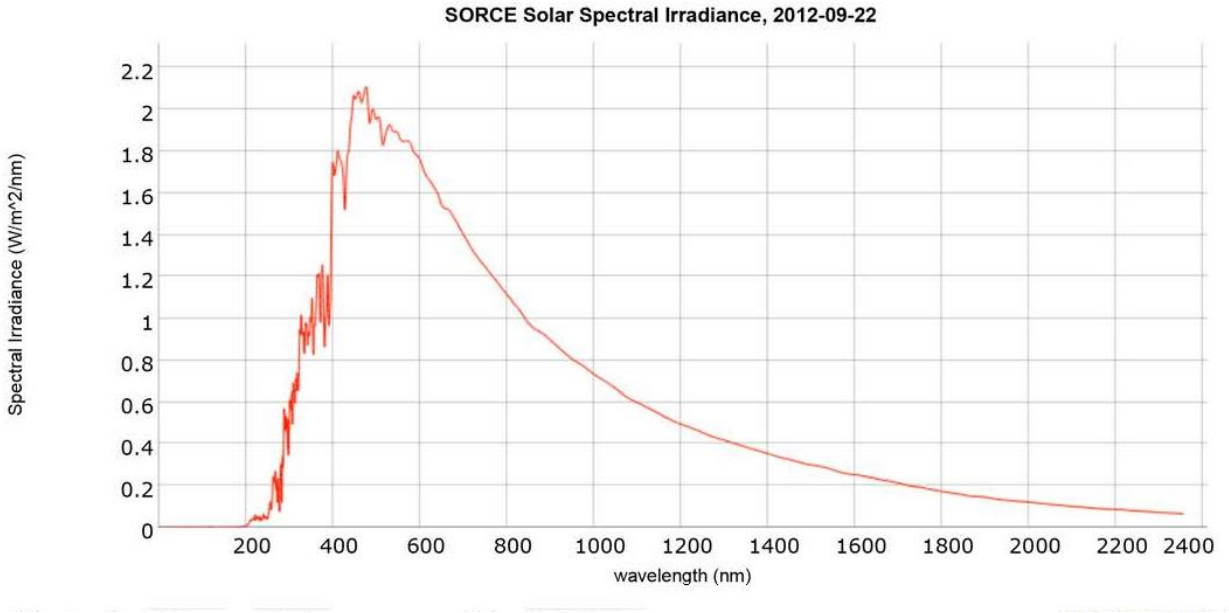

Figure 11 : irradiance of sun light in wavelength range of 0.5 - 2412.34 (nm) on 09/22/2012

Figure 12 : irradiance of sun light in wavelength range of 450 - 500 (nm) on 09/22/2012

As it is clear in figure 12, it is more efficiently to design our Nantenna for 0.625 Peta Hertz frequencies (480 nm). Regarding to table 1, though the irradiance of UV from sun is less than infrared and visible light frequencies, the excess energy of photons in the UV frequency is greater than infrared or visible light frequencies and makes up for the lack of irradiance.

The challenge here is to build Nantenna small enough to collect the energy of mentioned photons since frequency and Nantenna size have reverse relation, the higher the frequency is, the smaller the antenna should be [27], [28]. By choosing the desired frequency, the size of Nantenna will be calculated. The relation can be shown as:

$$f = \frac{c}{2\pi r} \qquad \text{(Equation 61)}$$

Where "f" is frequency (Hz), "C" is the speed of light (3×108 m/s) and "r" is radius of spiral Nantenna. According to radius size of Nantenna, we can estimate the radius of CNT. So we can find the chiral vector from equations 5, 6 and 11. Finding chiral vector leads to find the conductivity of Nantenna (using equations 62, 63, 64 and 65).

The efficiency of energy conversion through this method is far better than conventional PV panels since the ratio of output energy over Sun's energy is much greater. In addition, the energy efficiency of the systems that this technique may be used for can be improved using methods [29]–[31].

Another application of such structure is tangible in biomedical area. The benefits of nanotechnology in medical applications are enormous. Numerous research groups [32]–[35]have investigated the use of nanoparticles not only in medicines, but also medical devices so they can increase the effect of healing and remission. For instance, it can be used to guide the synthesis of nanowires based nanostructured antenna. Drug delivery is another application of such structures.

The last application of the proposed energy harvesting system, could be in Internet Of the Thing (IOT) devices. These remote devices are constrained to have chips that consume as low power as possible, since they are located in places that are not easy for humans to live in (i.e. deserts) and it is preferred to lower the computation performance to save energy [36]–[40]. Having the proposed technique eases this need. Also, due to the nano-dimension of utilized antennas, the Power Delivery Network (PDN) on ASIC chips (which has the task of delivering a constant voltage all over the chip) could target to provide more voltage to area with higher voltage drop and mitigate the complication of PDN [38], [41], [42].

Chapter 4 CONCLUSION:

To sum up, in order to find the conductivity, first we should find “m” and “n” from the chiral vector, and then we can proceed as bellow:

$$\begin{cases} |P_{\emptyset}| = \frac{s}{m}\frac{2\pi\hbar}{\sqrt{3}a_0}, \quad s = 1,2,3,\dots,m \\ |P_z| < \frac{4\pi\hbar}{3a_0} - \frac{1}{\sqrt{3}}P_{\emptyset} \end{cases} \qquad \text{(Equation 62)}$$

$$\sigma_{zz}(\omega) = j\frac{2e^2}{(2\pi\hbar)^2}\sum_{p_{\emptyset}}\int_{first\ Brillion\ zone}\frac{\partial f_0(p)}{\partial p_z}\frac{\nu_z}{(\omega - j\vartheta)}dp_z \qquad \text{(Equation 63)}$$

Where:

$$f_0(p) = \left(1 + e^{\frac{E(p)-E_F}{k_B T}}\right)^{-1} \qquad \text{(Equation 64)}$$

And:

$$E_{(P)} = -\gamma\sqrt{1 + 4\cos^2(\frac{a_0}{2\hbar}P_z) + 4\cos(\frac{\sqrt{3}}{2\hbar}a_0 P_{\emptyset})\cos(\frac{a_0}{2\hbar}P_z)} \qquad \text{(Equation 65)}$$

As an example, for small radius CNT, (m<50), conductivity will approximately be [14], [43]:

$$\sigma_{cn}(\omega) = \sigma_{zz}(\omega) \cong -j\frac{2e^2\nu_F}{\pi^2\hbar a(\omega - j\nu)} \qquad \text{(Equation 66)}$$

Where "ν_F" is the Fermi velocity for CNT [14], [43].

According to the fact that CNT based Nantennas can harvest photon’s energy from higher frequency band, the output electrical energy via this method is greater than it from PV panels, in same time duration. In other word, the efficiency of CNT based Nantennas is far better. These Nantennas can be formed by scaffolding CNT over DNA structures. Since they also have DNA as part of their structure, they can be used for drug delivery application and cancer treatments as well.

Also other industry and research areas such as nano sensors and nano robots can use them in order to make efficiency higher.

References:

[1] F. D.-R. and S. E. Reviews and undefined 2011, “The analysis on photovoltaic electricity generation status, potential and policies of the leading countries in solar energy,” *Elsevier*.

[2] S. Shafiee, E. T.-E. policy, and undefined 2009, “When will fossil fuel reserves be diminished?,” *Elsevier*.

[3] I. K.-E. and Buildings and undefined 1999, “Utilization of wind energy in space heating and cooling with hybrid HVAC systems and heat pumps,” *Elsevier*.

[4] A. H.-R. and sustainable energy reviews and undefined 2008, “A key review on exergetic analysis and assessment of renewable energy resources for a sustainable future,” *Elsevier*.

[5] P. Crutzen, A. Mosier, … K. S.-A., and undefined 2007, “N2O release from agro-biofuel production negates global warming reduction by replacing fossil fuels,” *hal.archives-ouvertes.fr*.

[6] A. Bolonkin, J. F. -, undefined Energy, and E. Engineering, and undefined 2013, “Explosion of Sun,” *file.scirp.org*.

[7] P. M. Ajayan, “Nanotubes from Carbon,” *Chem. Rev.*, vol. 99, no. 7, pp. 1787–1800, Jul. 1999.

[8] E. A. Rohlfing, D. M. Cox, and A. Kaldor, “Production and characterization of supersonic carbon cluster beams,” *J. Chem. Phys.*, vol. 81, no. 7, pp. 3322–3330, Oct. 1984.

[9] T. E.-C. N. P. and Properties and undefined 1997, “Production and purification of carbon nanotubes,” *books.google.com*.

[10] M. Zhao, M. Yu, R. B.-I. J. of S. T. in, and undefined 2012, “Wavenumber-domain theory of terahertz single-walled carbon nanotube antenna,” *ieeexplore.ieee.org*.

[11] G. H.-A. and P. S. International and undefined 2005, “Fundamental transmitting properties of carbon nanotube antennas,” *ieeexplore.ieee.org*.

[12] P. Datta, “nanoHUB-U Fundamentals of Nanoelectronics.” [Online]. Available: www.nanohub.org.

[13] R. Saito, G. Dresselhaus, and M. Dresselhaus, *Physical properties of carbon nanotubes*. 1998.

[14] G. Y. Slepyan, S. A. Maksimenko, A. Lakhtakia, O. Yevtushenko, and A. V. Gusakov, “Electrodynamics of carbon nanotubes: Dynamic conductivity, impedance boundary conditions, and surface wave propagation,” *Phys. Rev. B*, vol. 60, no. 24, pp. 17136–17149, Dec. 1999.

[15] J. Shi, A. R. Votruba, O. C. Farokhzad, and R. Langer, “Nanotechnology in Drug Delivery and Tissue Engineering: From Discovery to Applications,” *Nano Lett.*, vol. 10, no. 9, pp. 3223–3230, Sep. 2010.

[16] J. W.-M. device technology and undefined 2003, “Nanotechnology applications in medicine.,” *europepmc.org*.

[17] J. B. Falabella, T. J. Cho, D. C. Ripple, V. A. Hackley, and M. J. Tarlov, “Characterization of Gold Nanoparticles Modified with Single-Stranded DNA Using Analytical

Ultracentrifugation and Dynamic Light Scattering," *Langmuir*, vol. 26, no. 15, pp. 12740–12747, Aug. 2010.
[18] G. Matyi, A. Csurgay, W. P.-C. and Systems, undefined 2006, and undefined 2006, "Nanoantenna design for THz-band rectification," *ieeexplore.ieee.org*.
[19] M. Mi, M. Mickle, … C. C.-I. antennas and, and undefined 2005, "RF energy harvesting with multiple antennas in the same space," *ieeexplore.ieee.org*.
[20] J. Hone, M. C. Llaguno, N. M. Nemes, A. T. Johnson, J. E. Fischer, D. A. Walters, M. J. Casavant, J. Schmidt, and R. E. Smalley, "Electrical and thermal transport properties of magnetically aligned single wall carbon nanotube films," *Appl. Phys. Lett.*, vol. 77, no. 5, pp. 666–668, Jul. 2000.
[21] J. Le, Y. Pinto, N. Seeman, K. M.-F.-N. Letters, and undefined 2004, "DNA-templated self-assembly of metallic nanocomponent arrays on a surface," *ACS Publ.*
[22] C. Monson, A. W.-N. letters, and undefined 2003, "DNA-templated construction of copper nanowires," *ACS Publ.*
[23] E. Braun, Y. Eichen, U. Sivan, G. B.-Y.- Nature, and undefined 1998, "DNA-templated assembly and electrode attachment of a conducting silver wire," *nature.com*.
[24] H. Maune, S. Han, R. Barish, … M. B.-N., and undefined 2010, "Self-assembly of carbon nanotubes into two-dimensional geometries using DNA origami templates," *nature.com*.
[25] A. Vakil and H. Bajwa, "Energy harvesting using Graphene based antenna for UV spectrum," in *LISAT*, 2014.
[26] University of Colorado, "LISIRD." [Online]. Available: http://lasp.colorado.edu/lisird/. [Accessed: 26-Jan-2012].
[27] A. Vakil, A. Alsharani, C. Bach, J. Pallis, and H. Bajwa, "Fabrication and Mathematical Modeling of SWCNT Scaffold DNA Spiral Nantenna," 2015.
[28] A. Vakil and H. Bajwa, "Analytical model of Graphene based antenna for energy harvesting applications," in *ASEE*, 2014.
[29] S. Shahosseini, K. Moazzemi, A. M. Rahmani, and N. Dutt, "Dependability evaluation of SISO control-theoretic power managers for processor architectures," *Nord. Circuits Syst. Conf. NORCHIP Int. Symp. Syst.*, pp. 1–6, 2017.
[30] S. Shahhosseini, K. Moazzemi, A. M. Rahmani, and N. Dutt, "On the feasibility of SISO control-theoretic DVFS for power capping in CMPs," *Microprocess. Microsyst.*, vol. 63, pp. 249–258, 2018.
[31] A. M. Rahmani, B. Donyanavard, T. Müch, K. Moazzemi, A. Jantsch, O. Mutlu, and N. Dutt, "SPECTR: Formal Supervisory Control and Coordination for Many-core Systems Resource Management," *Proc. Twenty-Third Int. Conf. Archit. Support Program. Lang. Oper. Syst.*, pp. 169–183, 2018.
[32] J. N. ANKER, W. P. HALL, O. LYANDRES, N. C. SHAH, J. ZHAO, and R. P. VAN DUYNE, "Biosensing with plasmonic nanosensors," in *Nanoscience and Technology*, Co-Published with Macmillan Publishers Ltd, UK, 2009, pp. 308–319.
[33] J. Haun, N. Devaraj, S. Hilderbrand, … H. L.-N., and undefined 2010, "Bioorthogonal chemistry amplifies nanoparticle binding and enhances the sensitivity of cell detection," *nature.com*.
[34] C. Loo, A. Lin, L. Hirsch, M.-H. Lee, J. Barton, N. Halas, J. West, and R. Drezek, "Nanoshell-Enabled Photonics-Based Imaging and Therapy of Cancer," *Technol. Cancer Res. Treat.*,

vol. 3, no. 1, pp. 33–40, Feb. 2004.
[35] X. Shi, S. Wang, S. Meshinchi, M. E. Van Antwerp, X. Bi, I. Lee, and J. R. Baker, "Dendrimer-Entrapped Gold Nanoparticles as a Platform for Cancer-Cell Targeting and Imaging," *Small*, vol. 3, no. 7, pp. 1245–1252, Jul. 2007.
[36] H. M. Makrani, H. Sayadi, D. Motwani, H. Wang, S. Rafatirad, H. Homayoun, "Energy-aware and Machine Learning-based Resource Provisioning of In-Memory Analytics on Cloud," *Proc. ACM Symp. Cloud Comput.*, 2018.
[37] H. M. Makrani, S. Tabatabaei, S. Rafatirad, H. Homayoun, "Understanding the role of memory subsystem on performance and energy-efficiency of Hadoop applications," *IGSC*, 2017.
[38] A. Vakil, H. Homayoun, and A. Sasan, "IR-ATA: IR annotated timing analysis, a flow for closing the loop between PDN design, IR analysis & timing closure," in *ASP-DAC*, 2019.
[39] M. Daneshzand, S. A. Ibrahim, M. Faezipour, and B. D. Barkana, "Desynchronization and Energy Efficiency of Gaussian Neurostimulation on Different Sites of the Basal Ganglia," *2017 IEEE 17th International Conference on Bioinformatics and Bioengineering (BIBE)*, 2017
[40] M. Daneshzand, D. Thomas, K. Elleithy, and M. Faezipour, "An energy efficient wireless sensor network based on human neurons communication," *2015 IEEE International Conference on Multisensor Fusion and Integration for Intelligent Systems (MFI)*, 2015.
[41] N. Sehatbakhsh, A. Nazari, A. Zajic, and M. Prvulovic, "Spectral profiling: Observer-effect-free profiling by monitoring EM emanations," *Int. Symp. Microarchitecture*, p. 59, 2016.
[42] M. Dey, A. Nazari, A. Zajic, M. Prvulovic "EMPROF: Memory Profiling Via EM-Emanation in IoT and Hand-Held Devices," 2018 International Symposium on Microarchitecture (MICRO), pp. 881-893.
[43] S. Maksimenko, … G. S. in unconventional materials, and undefined 2000, "Electrodynamic properties of carbon nanotubes," *New York Wiley*.
[44] "nanohubtechtalks." [Online]. Available: https://www.youtube.com/channel/UCf5RZWvpGU0RTBhXBMrc0jw.
[45] R. Pierret and G. Neudeck, *Advanced semiconductor fundamentals*. 1987.
[46] K. Iniewski and J. Morris, *Graphene, carbon nanotubes, and nanostructures: techniques and applications*. 2016.

Appendix A : MATLAB Codes

MATLAB code:

The energy band can be plotted in MATLAB with this code:

>>>

```
a=(sqrt(3)*1.42);
x= linspace(-pi,pi);
y= linspace(-pi,pi);
[x,y]= meshgrid(x,y);
z=(-2.7)*(sqrt(1+(4*(cos(((sqrt(3))/2).*a.*x)).*(cos((a.*y)/2)))+(4*((cos((a.*y)/2)).^2))));
mesh(x,y,z)
```

<<<

APPENDIX B : CONFERENCE PAPER

Energy Harvesting Using Graphene Based Antenna for UV Spectrum

Askhan Vakil
Department of Electrical Engineering
221 University Ave, University of Bridgeport,
Bridgeport, CT.

Hassan Bajwa
Department of Electrical Engineering
221 University Ave, University of Bridgeport,
Bridgeport, CT.

Abstract— **Recent advances in the fabrication and characterization of nanomaterials have led to the intelligible applications of such nanomaterials in the next generation of flexible electronics and highly efficient photovoltaic devices. Nanotechnology has been used in thin film photovoltaic devices, and is considered as one of the most promising research areas in power harvesting applications. The excellent electron transport properties of Graphene make it an attractive choice for the next generation of electronics and applications in energy-related areas. In this paper, we present the design and an analytical model of graphene-based nanoscale antennas for power harvesting applications. Unlike conventional solar cells that harvest energy in the visible light frequencies range, we focus on the design of a nanoscale antenna that harvests energy in the UV spectrum range frequencies. Though the irradiance of UV from the sun is less than infrared and visible light frequencies, the excess energy of photons in the UV frequency is greater than infrared or visible light frequencies and makes up for the lack of irradiance.**

Keywords-component; Nanoantenna; Graphene based antenna; Energy harvesting; Patch antenna; Solar energy, UV frequency (key words)

I. INTRODUCTION

Advances in nanotechnology have led to the development of semiconductor based solar cells, nanoscale antennas for power harvesting applications [1-3] and integration of antennas into solar cells to design low-cost light weights systems [2, 4]. Similarly, Grapheme has emerged as a promising candidate for the next generation and post silicon electronics. Graphene based antennas have been explored due to the high optical transmittance and conductivity of Graphene [5]. In this paper, we present the design and analytical model of Graphene based antenna for power harvesting application. Typically, solar cells use the visible light to produce electricity, the photovoltaic and rectification properties of sandwiched material are used to produce electricity. Unlike conventional solar cells that harvest energy in visible light frequency range, we focus on the design of graphene based nanoscale antenna in the UV spectrum range frequencies. Since the UV frequency range is much greater than visible light, we consider the quantum mechanical behavior of a driven particle in graphene to calculate the current in graphene based nanoscale antennas for power harvesting applications.

The sun is the biggest energy source for humankind, but taping into this huge energy reservoir remains a challenge. Solar energy is enormous. The surface of the earth receives about $3x10^{24}$ Joules per year [5]. The energy reaches the earth in the form of emitted photons with variant frequencies. The frequencies of these photons represent the wavelength spectrum of sunlight which vary from radio waves, to gamma waves. Sunlight, in space, contains about 50% infrared waves, 40% visible light and 10% UV, X and γ waves. Each wave has its own frequency range and these ranges define the energy of each wave. The energy of a photon with a specified frequency is defined as:

$$E=h\times f$$

where "h" is the Planks constant, "f" is the frequency of the wave and "E" is the energy of photon (Joules). There are many ways to harvest this energy from the Sun. In addition to conventional solar panels and solar-water heaters, antennas are emerging as a promising technology for light energy harvesting [6] tools.

Solar plants use different ways to harvest energy from the sun. Some plants use the heat (infrared photons) and concentrate it on a specific point (boiler) to heat up water for the steam turbine in power plants. Such solar cells use the visible light to produce electricity. Other panels use heat to produce the air flow in towers and use wind turbines to produce power.

II. SOLAR PANELS AND ANTENNAS:

Typically, solar cells consist of a semiconductor as a middle layer surrounded by two conductive layers. They use the photo-electric phenomenon to produce electricity [7]. Working at the visible light frequency, these solar cells excite an electron and move it to the valance shell. Such solar cells employ p-n junctions in semiconductor and the current flow as electrons flows across the p-n junctions. Photovoltaic panels can be connected in series or parallel to get the desired output voltage or current. Contrary to classical solar cells (Fig 1), the antenna based solar cells use Faradays law to produce the current. They are mostly made of copper, since copper has a good conductivity and their structure is easier than solar cells.

Published in: Systems, Applications and Technology Conference (LISAT), 2014 IEEE Long Island, 2 May 2014, Farmingdale, NY, USA

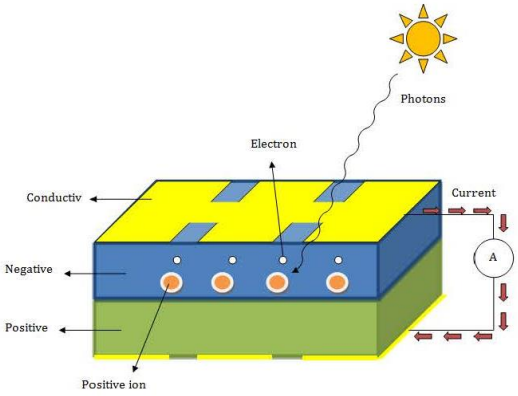

Figure 1: Solar Cells

The theoretical efficiency of antenna based solar cells is greater than conventional solar cells. Antennas, in the energy harvesting area, are mostly designed for Infrared waves. Although Infrared waves have less energy than the visible light or UV, since sunlight mostly consist of infrared waves, the power which is harvested is significant. The amount of UV waves in space is greater than Earth's. The reason is that the ozone layer filters out the frequencies higher than the visible light. In this paper, we propose using Graphene to build antennas and gather the energy from UV waves in space.

III. WHY UV

Traditional photovoltaic (PV) solar cells harvest energy from the visible and the infrared light spectrum. Despite the improvement in the semiconductor industry, PV solar cells are not efficient, as they do not absorb long and short wavelength lights [2]. While irradiance of UV light is much lower than visible light (Figure 2), power per photons due to the extremely large frequency is much more than the visible and infrared frequencies. UV waves have a frequency range between 0.75 PHz and 3 PHz. The frequencies above 1.034 PHz are being absorbed by the ozone layer. These photons may cause cancer and they have a great amount of energy. Quantum mechanics states that the frequency and energy of a quantum of electromagnetic radiation are proportional. A photon with the frequency higher than the threshold frequency of a matter will excite the electron to jump out from an atom. The Photons with visible light frequency can excite the electrons from atoms of some materials. This process is being used in solar cells to produce an electrical current. Since the UV frequency range is much greater than visible light, not only does it excite electrons to the Valance shell and makes the antenna more conductive, but it will also give the electrons enough energy to increase this current. As we know from quantum mechanics, if the frequency of a photon is more than the minimum threshold frequency, it can excite an electron and release it from its atom:

$$K = hf_{ph} - hf_0$$

f_0 is the threshold frequency of matter.

Table 1: Energy of photons and corresponding frequencies:

Wave	Frequency range	Energy of a photon (eV)
Infrared	0.3THz – 0.429 PHz	0.001 – 1.772
Visible-Light	0.385PHz – 0.789 PHz	1.591 – 3.265
UV-A	0.75 PHz – 0.952 PHz	3.102 – 3.939
UV-B	0.952 PHz – 1.07 PHz	3.939 – 4.431
UV-C	1.07 PHz – 1.5 PHz	4.431 – 6.203
Vacuum UV	1.5 PHz – 3 PHz	6.203 – 12.407

Table 1: Energy of photons with different frequencies

The average photon energy (APE) indicates a spectral irradiance distribution. APE expresses the relationship between the average photon flux density and irradiance[8]. Photon flux shows the number of photons that hit the unit surface per second. We can find the total energy in each wavelength from the energy and flux density. The relationship between the photon flux and irradiance is as below:

$$H = \Phi \times E = \Phi \times h \times f$$

Where H is the irradiance (W/m^2), Φ is the photon flux (number of photons/sm^2), E is energy of the photon (J), h is the Plank constant and f is the frequency (Hz).

The irradiance of sunlight can be plotted in the figure 2 below:

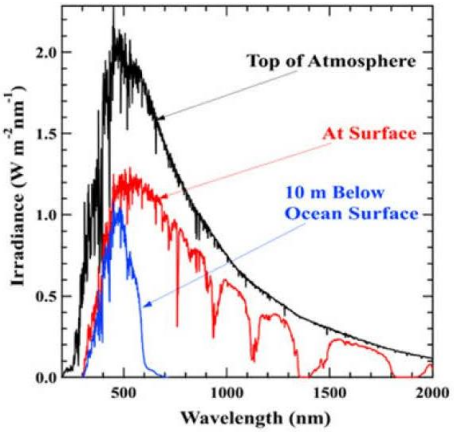

Figure 2: The irradiance of sunlight

We used the data from "Solar Radiation and Climate Experiment" (SORCE) [9, 10] to build the relationship between the photon flux and irradiance. Irradiances are reported by Solar Spectral Irradiance (SSI) at a mean solar distance of 1 astronomical unit (AU) with units of W/m2/nm. Figure 3 and 4 are the data collected on September 29th of 2009:

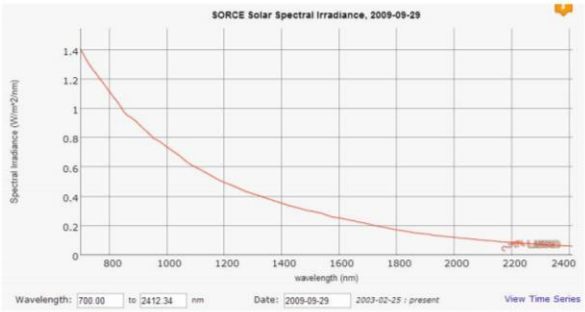

Figure 3: Infrared irradiance on 9-29-2009, collected by SSI

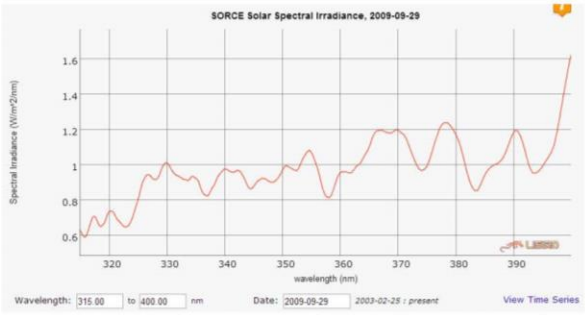

Figure 4: UVA irradiance on 9-29-2009, collected by SSI

It is important to emphasize the fact that these irradiances are presenting the irradiance in space which is the reason of high amount of UV irradiance.

Table 2 Energy in UV, UAV and Infrared bands

Wave		λ (nm)	H (W/m^2)	Φ ($Photons/sm^2$)	E per Photon (eV)	E Total (eV/sm^2)
Infrared	Max	2412.34	0.060679	7.36384E+17	0.51430858	3.78729E+17
	Min	701.56	1.4017	4.94706E+18	1.768469068	8.74872E+18
UVA	Max	400.34	1.6641	3.35147E+18	3.099083676	1.03865E+19
	Min	315.02	0.63217	1.00184E+18	3.938439334	3.94569E+18
UVB	Max	315.02	0.93217	1.47727E+18	3.938439334	5.81815E+18
	Min	280.5	0.086971	1.22725E+17	4.423127127	5.4283E+17

Table 2 shows the energy per photon as well as the total energy in UV, UAV and Infrared bands. By comparing the total energy of infrared and UVA waves in the table, we see that the maximum energy in UVA is greater than infrareds energy.

IV. Electrical and Chemical Properties of Graphene

Carbon is located in group IV of the periodic table, which means that Carbon has four valance electrons. Carbon forms different allotropes such as graphite, diamond and graphene. In graphene, all the carbon atoms form covalent bonds. It is a monolayer honeycomb lattice structure. Graphene Nanoribbons (GNR) can be formed by cutting graphene sheets in small rectangles. GNR exhibit excellent electrical, optical, mechanical, thermal and quantum-mechanical properties[11, 12]. The practical threshold frequency of graphene is 1 THz. Calculating the k value from the quantum mechanics equation, we can see that K is a positive value, which means the photons with a UV frequency can excite electrons from atoms:

$$K_{graphene} = h(f_p - f_0) = 4.135\times10^{-15}\times(1P - 1T) = 4.1309\ e.V$$

Thus, a graphene based patch antenna shown in figure 5 will exhibit excellent properties and can be used to produce a high amount of current.

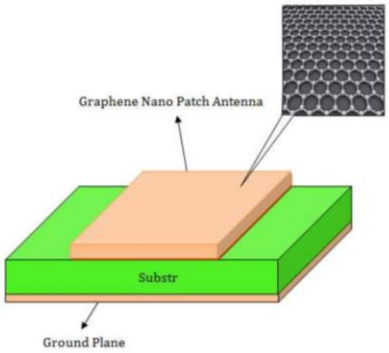

Figure 5: Graphene based patch antenna for power harvesting applications

V. Array Nano Patch Antennas using Graphene:

We have proved analytically that graphene based patch antenna can be used to harvest energy from the UV spectrum. Due to the higher energy of the UV photons, the free electrons of a single layer graphene not only gain this energy, but also the electrons in 2s shell of carbon atoms (first layer) can be excited and move to the valance layer. Therefore, the number of electrons in the valance layer increases and so does the current. Like other harvesting systems that use nanoantennas [1, 2], in order to increase the output, we should design more than one single nano-patch antenna. Array of antennas with an integrated rectifier circuit have been reported in the literature [1, 2]. The rectifier circuits can be used to convert these high frequency output currents into a useable current. For this, we need a diode that works in Petahertz frequency. High frequency metal-insulator -metal (MIM) diodes can be used to build a rectifier kit. These diodes are also made from graphene.

VI. Results

Conventional solar cells have very low efficiency [13], the most expensive solar cells reach up to 30% efficiency. Even with the advances in nano-technology, current solar cell technology has little chance to compete with fossil fuels.

ientists are investigating various nano-structures and their signs to harvest energy from various frequencies of light l]. In this paper, we presented a design and an analytical odel for MIM tunneling diode with an integrated graphene sed patch antenna.

The applications of such antennas are in the field of power rvesting and aerospace industry [15]. We calculated and mpared the energy of photons in Infrared, UV and visible ht spectrums. We concluded that light weight, highly icient graphene based nanoscale antennas can be designed to rvest energy from the UV light spectrum.

REFERENCES

[1] D. K. Kotter, S. D. Novack, W. D. Slafer, and P. Pinhero, "Solar nantenna electromagnetic collectors," in *ASME 2008 2nd International Conference on Energy Sustainability collocated with the Heat Transfer, Fluids Engineering, and 3rd Energy Nanotechnology Conferences*, 2008, pp. 409-415.

[2] R. Corkish, M. A. Green, and T. Puzzer, "Solar energy collection by antennas," *Solar Energy,* vol. 73, pp. 395-401, 2002.

[3] K. Shankar, J. Bandara, M. Paulose, H. Wietasch, O. K. Varghese, G. K. Mor, T. J. LaTempa, M. Thelakkat, and C. A. Grimes, "Highly efficient solar cells using TiO2 nanotube arrays sensitized with a donor-antenna dye," *Nano letters,* vol. 8, pp. 1654-1659, 2008.

[4] N. Henze, M. Weitz, P. Hofmann, C. Bendel, J. r. Kirchhof, and H. Fruchting, "Investigation of planar antennas with photovoltaic solar cells for mobile communications," in *Personal, Indoor and Mobile Radio Communications, 2004. PIMRC 2004. 15th IEEE International Symposium on*, 2004, pp. 622-626.

[5] X. Wang, L. Zhi, and K. MÃ¼llen, "Transparent, conductive graphene electrodes for dye-sensitized solar cells," *Nano letters,* vol. 8, pp. 323-327, 2008.

[6] M. W. Knight, H. Sobhani, P. Nordlander, and N. J. Halas, "Photodetection with active optical antennas," *Science,* vol. 332, pp. 702-704.

[7] M. Sarehraz, K. Buckle, T. Weller, E. Stefanakos, S. Bhansali, Y. Goswami, and S. Krishnan, "Rectenna developments for solar energy collection," in *Photovoltaic Specialists Conference, 2005. Conference Record of the Thirty-first IEEE*, 2005, pp. 78-81.

[8] T. Minemoto, S. Nagae, and H. Takakura, "Impact of spectral irradiance distribution and temperature on the outdoor performance of amorphous Si photovoltaic modules," *Solar energy materials and solar cells,* vol. 91, pp. 919-923, 2007.

[9] C. A. Gueymard, "The sun's total and spectral irradiance for solar energy applications and solar radiation models," *Solar Energy,* vol. 76, pp. 423-453, 2004.

[10] SCORE. (2003- 2013). *http://lasp.colorado.edu/sorce/data_access.html*.

[11] A. N. Grigorenko, M. Polini, and K. S. Novoselov, "Graphene plasmonics," *Nature photonics,* vol. 6, pp. 749-758.

[12] P. Avouris, Z. Chen, and V. Perebeinos, "Carbon-based electronics," *Nature nanotechnology,* vol. 2, pp. 605-615, 2007.

[13] B. O'regan and M. Grfitzeli, "A low-cost, high-efficiency solar cell based on dye-sensitized," *nature,* vol. 353, pp. 737-740, 1991.

[14] G. Matyi, A. I. Csurgay, and W. Porod, "Nanoantenna Design for THz-band Rectification," in *49th IEEE International Midwest Symposium on Circuits and Systems*, 2006, pp. 197-199.

[15] A. R. Jha, "MEMS and Nanotechnology-Based Sensors and Devices for Communications, Medical and Aerospace Applications.," 2008.